Low-Valent Uranium (2)

DOI: 10.1002/ange.201402050

Synthesis and Characterization of a Uranium(II) Monoarene Complex Supported by δ Backbonding**

*Henry S. La Pierre, Andreas Scheurer, Frank W. Heinemann, Wolfgang Hieringer, and Karsten Meyer**

Abstract: *The low-temperature ($< -35\,^{\circ}C$) reduction of the trivalent uranium monoarene complex $[\{(^{Ad,Me}ArO)_3mes\}U]$ (**1**), with potassium spheres in the presence of a slight excess of 2.2.2-cryptand, affords the quantitative conversion of **1** into the uranium(II) monoarene complex $[K(2.2.2\text{-crypt})][((^{Ad,Me}ArO)_3mes)U]$ (**1-K**). The molecular and electronic structure of **1-K** was established experimentally by single-crystal X-ray diffraction, variable-temperature ^1H NMR and X-band EPR spectroscopy, solution-state and solid-state magnetism studies, and optical absorption spectroscopy. The electronic structure of the complex was further investigated by DFT calculations. The complete body of evidence confirms that **1-K** is a uranium(II) monoarene complex with a $5f^4$ electronic configuration supported by δ backbonding and that the nearly reversible, room-temperature reduction observed for **1** at −2.495 V vs. Fc/Fc^+ is principally metal-centered.*

The rich redox chemistry of uranium and the middle actinide (U–Am) elements stands in stark contrast to the more limited redox chemistry of the early actinides and the lanthanides.[1] This dichotomous behavior is often attributed to the decrease in energy of the 5f orbitals across the actinide series and the small gap between the 5f orbitals and the 6d orbitals (ca. 300 cm^{-1} between U and Am).[1,2] In the lanthanides, the analogous gap between the 4f and 5d orbitals is greater (ca. 200 to 20000 cm^{-1} increasing from left to right),[1,3] and consequently, in conjunction with the smaller radial extent of the 4f orbitals, the redox chemistry of the lanthanides is significantly more limited. The identification and comprehensive analysis of a new, low-valent uranium oxidation state provides a tool to probe these key aspects of orbital energy and radial extent necessary to understand the redox behavior and electronic structure of the middle actinide (U–Am) elements.

Divalent uranium has previously been identified in a neon or argon matrix in the reaction of U with CO_2 to give OUCO and in the reaction of U with S to give molecular US.[4] Additionally, potential formal divalent uranium has been identified in the solid-state material US.[5] However, the magnetic properties of this material suggest that electrons are delocalized in the conduction band. Gas-phase experimental data and calculations indicate that for U^{2+} the $5f^4$ configuration is slightly (210 cm^{-1}) lower in energy than the $5f^3\,6d^1$ configuration for the free ion.[2a–c] Given the small splitting between the d and f orbitals for atomic U^{2+}, the ligand sphere in a potential molecular complex is expected to play a dominant role in determining the ground-state electronic structure.

Synthetic studies aiming to identify a molecular, divalent uranium complex have been pursued since at least 1980.[6] Early studies established that $[\{Cp^*{}_2UCl\}_3]$, $Na[Cp^*{}_2UCl_2]$, and $[Cp^*{}_3U]$ can serve as synthetic equivalents for the divalent complex $[Cp^*{}_2U]$ under appropriate conditions ($Cp^* = C_5Me_5$).[7] However, no spectroscopic, crystallographic, or electrochemical evidence for such a divalent intermediate species was ever obtained.[7c,8] In 2000, a new structural motif in uranium chemistry was identified with the isolation of the diuranium, inverted arene complexes $[\{(Ar(R)N)_2U\}_2(\mu^2\text{-}\eta^6{:}\eta^6\text{-arene})]$ ($R = t$Bu or Ad, $Ar = 3,5\text{-}C_6H_3Me_2$) and $[\{(Cp^*{}_2U\}_2(\mu^2\text{-}\eta^6{:}\eta^6\text{-}C_6H_6)]$.[9] One possible formulation of these complexes includes the assignment of the formal oxidation state of two uranium(II) centers and a bridging neutral arene.[10] While synthetic studies indicated that these complexes could behave as four-electron reductants, subsequent, elaborate spectroscopic studies have established that the complexes incorporate two uranium centers, each with two solely f electrons, and a bridging, diamagnetic arene tetraanion which binds through covalent δ bonds to each uranium center, thus giving a resultant spectroscopic oxidation state at each U ion of U^{3+}.[11]

Recent work has expanded the known canonical oxidation states of the lanthanides[3b,12] by extending the methodology for the isolation of the elusive thorium(III) oxidation state in $[(Cp(1,3\text{-}SiMe_3))_3Th]$[13] to the reduction of derivatized *tris*-Cp (Cp = cyclopentadienide) complexes of trivalent lanthanides. This coordination geometry seems to favor a $4f^n\,5d^1$ electronic configuration with the added electron residing in a d_{z^2} orbital to decrease interaction with the equatorial ligand

---

[*] Dr. H. S. La Pierre, Dr. A. Scheurer, Dr. F. W. Heinemann, Prof. Dr. K. Meyer
Inorganic Chemistry, Department of Chemistry and Pharmacy, Friedrich-Alexander University Erlangen-Nürnberg
Egerlandstrasse 1, 91058 Erlangen (Germany)
E-mail: karsten.meyer@fau.de

Priv.-Doz. Dr. W. Hieringer
Theoretical Chemistry, Department of Chemistry and Pharmacy, Friedrich-Alexander University Erlangen-Nürnberg
Egerlandstrasse 3, 91058 Erlangen (Germany)

[**] We would like to thank Prof. Dr. R. Wolf and Dr. B. Rad for the donation of [K(18-C-6)][Cp*Fe(napth)] as a possible outer sphere reductant for **1**. The Bundesministerium für Bildung und Forschung (BMBF 2020+, 02NUK012C and 02NUK020C), the FAU Erlangen-Nürnberg, COST Action (CM1006), and the Cluster of Excellence “Engineering of Advanced Materials” are acknowledged for financial support.

Supporting information for this article is available on the WWW under http://dx.doi.org/10.1002/anie.201402050.

sphere. Applying this approach to uranium has resulted in the isolation of a U^{2+} complex with a $5f^36d^1$ ground state as assigned by XRD, UV/vis, and TD-DFT.[14]

Our approach employs a chelating tris(aryloxide) arene uranium(III) complex, [{(^{Ad,Me}ArO)$_3$mes}U] (**1**).[15] This chelating ligand system enables δ backbonding between uranium and the arene and solubilizes the monoarene complex.[16] We have previously shown that derivatives of the uranium(III) monoarene complex **1** engage in two covalent δ bonds with the π^* orbitals of the arene base, each partially occupied with a single electron.[17]

The nearly reversible reduction observed for **1** at −2.495 V vs. Fc/Fc$^+$ at room temperature suggested that this initial reduction product could be isolated and fully characterized under appropriate conditions.[15] To this end, it was found that adding potassium spheres to a chilled (−35 °C) deep purple solution of **1** and 2.2.2-cryptand in THF and allowing it to stand overnight (12–15 h) at −35 °C, led to quantitative conversion into a single new, deep red/brown species, namely [K(2.2.2-crypt)][((^{Ad,Me}ArO)$_3$mes)U] (**1-K**; Scheme 1).

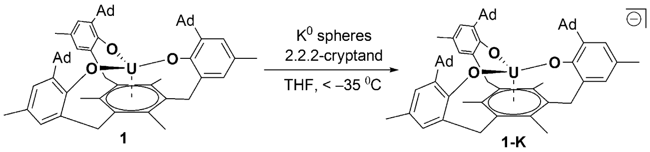

Scheme 1. Synthesis of the anion of **1-K**.

Executing this procedure in [D$_8$]THF, followed by rapid decantation from the potassium into a pre-chilled (approx. −100 °C) J. Young tap NMR tube and, in turn, rapid introduction to a prechilled (−40 °C) spectrometer, allowed for variable-temperature ^{1}H NMR measurements. These studies confirmed the quantitative formation of a single new, C_3-symmetric complex, **1-K** (Figure 1 and Figures S1, S3, and S4 in the Supporting Information). The spectrum of **1-K** at −40 °C features nine resonances, which are attributable to the uranium anion [((^{Ad,Me}ArO)$_3$mes)U]$^-$, between $\delta = 27.65$ and −6.10 ppm and three broad resonances for the cation [K(2.2.2-crypt)]$^+$ (one of which overlaps with the anion resonances).[18] Warming a solution of **1-K** to room temperature leads to the rapid conversion (< 10 min. in solution, < 3 h in solid-state) into a previously characterized arene functionalized product (**2**), as determined by ^{1}H NMR spectroscopy and XRD (see Figures S2 and S15 in the Supporting Information).[15] Having demonstrated the quantitative conversion into **1-K** in solution below −35 °C, qualitative UV/vis spectra were recorded for **1** and **1-K** between $\lambda = 400$ and 1650 nm (see Figure S5 in the Supporting Information). Upon reduction, the fine structure observed for **1** is lost and a single broad absorbance at ca. $\lambda = 600$ nm is observed with weak f–f transitions observed between $\lambda = 1100$ and 1650 nm (see Figure S6 in the Supporting Information).

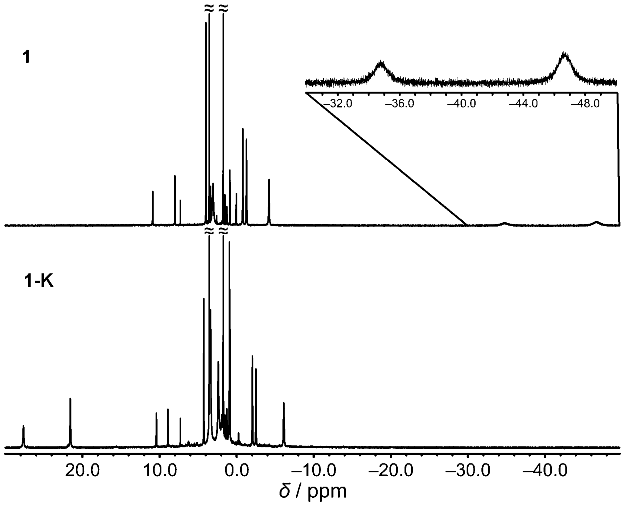

Figure 1. ^{1}H NMR spectra of **1** (top) and **1-K** (bottom) in [D$_8$]THF at −40 °C.

To gain further insight into the molecular and electronic structure **1-K**, its solid-state molecular structure was determined by X-ray diffraction of crystals of **1-K**·$C_4H_{10}O$ (Figure 2a and Table 1). These crystals were obtained by the diffusion of diethyl ether into a 1:1 THF/DME solution of **1-K** at −35 °C. The complex **1-K**·$C_4H_{10}O$ crystallizes in the cubic space group $P2_13$ with both the complex anion and cation lying on crystallographic threefold axes. The molecular structure of the anion [{(^{Ad,Me}ArO)$_3$mes}U]$^-$ in **1-K** is very nearly superimposable with [{(^{Ad,Me}ArO)$_3$mes}U] in the molecular structure of **1** (Figure 2b).[15] In comparison to the room temperature chemical reduction of **1**, the benzylic C−C bonds of **1-K** are identical to those in **1** (1.515(7), 1.536(7), and 1.497(8) Å) and are not shortened (which would be indicative of H-atom rearrangement). Additionally, the

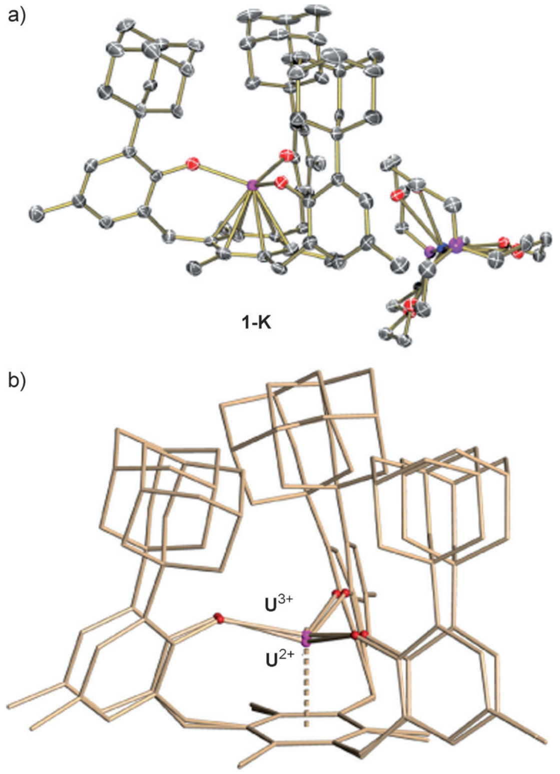

Figure 2. a) ORTEP representation of **1-K** with thermal ellipsoids at 50% in crystals of **1-K**·$C_4H_{10}O$ with hydrogen atoms and cocrystallized solvent removed for clarity.[28] b) Overlay of [{(^{Ad,Me}ArO)$_3$mes}U]$^-$ in **1-K** and [{(^{Ad,Me}ArO)$_3$mes}U] in **1**.[15]

Table 1: Selected bond lengths [Å] and angles [°] of **1**,[15] **1-K**, and $\mathbf{1}^{-}$.

	1 (XRD)	**1-K** (XRD)	$\mathbf{1}^{-}$ (Calc.)[b]
U–O	2.158(2), 2.169(2), 2.178(2)	2.236(4)	2.233
U–$\mathrm{C_{arene}}$	2.729(3), 2.732(3), 2.737(3), 2.755(3), 2.767(3), 2.774(3)	2.597(5), 2.633(5)	2.639, 2.640, 2.640, 2.688, 2.689, 2.689
$\mathrm{C_{arene}}$–$\mathrm{C_{arene}}$	1.418(5), 1.425(5), 1.428(4), 1.417(5), 1.420(5), 1.428(5)	1.432(7), 1.432(8)	1.433, 1.439
$\mathrm{C_{arene}}$–$\mathrm{C_{benzyl}}$	1.529(5), 1.528(4), 1.523(5)	1.515(7)	1.524
$\mathrm{U_{oop}}$[a]	0.475(2)	0.668(2)	0.627
U–Cent.	2.35	2.18	2.24
∡O-U-O	114.57(9), 113.91(9), 117.51(9)	111.49(8)	112.4, 112.4, 112.5

[a] Distance of U from the plane defined by the three O atoms along the normal. [b] Scalar-relativistic DFT calculations with the BP functional in $m_S = 2$ configuration.

uranium is centrally located between the aryloxide arms with a O-U-O angle of 111.49(8)°. Arene bonding is undisturbed in **1-K**: the arene carbon atoms are planar and the C–C bond is 1.432(7) Å, which is only 0.01 Å longer than that in the U^{3+} precursor **1** (1.42 Å (avg.)).

In contrast to the molecular structure of **1** and, most importantly, indicative of a metal-centered reduction, the uranium out-of-plane shift increases from 0.475(2) to 0.668(2) Å for **1-K**. This change is also reflected in the U–O bond lengths. In **1-K**, the U–O bond length increases to 2.236(4) Å in comparison to 2.168(2) Å (avg.) for **1**. In line with the lengthening of the U–O bond in **1-K**, the U–C bond length and U–arene centroid distance contracts from 2.749(3) (avg.) and 2.35 Å in **1** to 2.615(5) (avg.) and 2.18 Å in **1-K**. This synergistic contraction of the U–arene centroid distance is indicative of the change in charge distribution between the uranium ion and the arene ligand upon reduction and could be indicative of slightly stronger covalent and/or ionic interaction in **1-K** than in **1**, a conclusion which is further supported by DFT calculations (see below).

To shed light on the electronic structure of **1** and its one-electron reduction product **1-K**, density functional calculations[19] on **1** and its monoanion $\mathbf{1}^{-}$ were performed. As a precaution, it should be noted that the electronic structure of actinide complexes, and in particular the prediction of spin density distributions, which are of crucial importance here, poses a difficult problem for present-day density functional approximations.[20] In addition, relativistic effects should be taken into account. Herein, we report results from scalar-relativistic calculations[21] as well as calculations including spin-orbit interactions[22] on **1** and one-electron reduced $\mathbf{1}^{-}$. To arrive at a picture as robust as possible, we have used and compared four different exchange-correlation functionals in the scalar-relativistic calculations (see the Supporting Information for computational procedures and additional results).[23] Noteworthy, while the results obtained with various functionals differ in details, the qualitative results are self-consistent. Hence, the results qualitatively hold for all functionals. The geometry-optimized structures and metrics shown here have been obtained from scalar-relativistic calculations using the BP functional, and the results obtained with the other functionals can be found in the Supporting Information.

In the scalar relativistic calculations, we have considered the anion $\mathbf{1}^{-}$ in two different electronic configurations, those featuring four ($m_S = 2$) and two ($m_S = 1$) excess electrons in the majority spin channel. The four highest occupied spin orbitals in the majority spin channel for the $m_S = 2$ configuration are depicted in Figure S20 in the Supporting Information. The two singly-occupied δ-bonding orbitals, which had been described earlier in similar η^6 arene complexes,[17a,24] can clearly be identified in $\mathbf{1}^{-}$ as well. Note that the corresponding partner orbitals in the minority spin channel (not shown in Figure S20) are unoccupied. Furthermore, Figure S20 shows two U-centered f orbitals, which are likewise singly occupied. In comparison, a corresponding calculation for neutral **1** shows a similar electronic structure, including both singly occupied δ-bonding orbitals, but only one singly occupied f orbital on U (not shown). In $\mathbf{1}^{-}$, the electronic structure obtained for the $m_S = 1$ configuration qualitatively differs from that of the $m_S = 2$ configuration in that the spin of one electron is flipped and one of the formerly empty δ-bonding spin orbitals becomes occupied, while one of the f orbitals becomes vacant instead.

Single-point test calculations on $\mathbf{1}^{-}$, using atomic positions from the XRD geometry of **1-K**, suggest that the $m_S = 2$ system is slightly lower in energy by 16–19 kJ mol^{-1} than the $m_S = 1$ system for all four functionals considered here (see the Supporting Information for details). Upon geometry optimization, the total energies of $\mathbf{1}^{-}$ in one of the two configurations ($m_S = 2$ and $m_S = 1$) in their respective optimized geometries become virtually the same (see the Supporting Information for details), that is, the two electronic configurations cannot be distinguished by the present density functional calculations on energetic grounds alone. Table 1 shows selected structural parameters obtained for $\mathbf{1}^{-}$ in the $m_S = 2$ configuration, thus resulting in satisfactory agreement with the experimental structure. Geometry optimizations of $\mathbf{1}^{-}$ in the $m_S = 1$ configuration result in structures, which agree less well with the experimental structure of **1-K** (see Table S5 and Figure S22 in the Supporting Information). In particular, the $m_S = 2$ configuration results in a largely planar structure of the η^6 arene ring, in agreement with the XRD structure of **1-K**, while the $m_S = 1$ configuration yields a significantly distorted arene ring (a norboradiene type structure; see Figure S22). Noteworthy, all calculations on $\mathbf{1}^{-}$ reproduce the observed shorter U–arene distance by about 0.1–0.2 Å upon reduction of **1** to **1-K**/$\mathbf{1}^{-}$ (see Tables S3 and S5 in the supporting Information).

To estimate the effect of spin-orbit coupling on the electronic structure of $\mathbf{1}^{-}$, we additionally performed two-component relativistic DFT calculations[22] on $\mathbf{1}^{-}$ and **1** with the heavy atom positions taken from the experimental XRD structures of **1-K** and **1** (see the Supporting Information for details). Representations of the highest occupied and lowest unoccupied spinors are shown in Figure 3a. These calculations all together support the electronic structure described above for the scalar-relativistic calculations of the $m_S = 2$

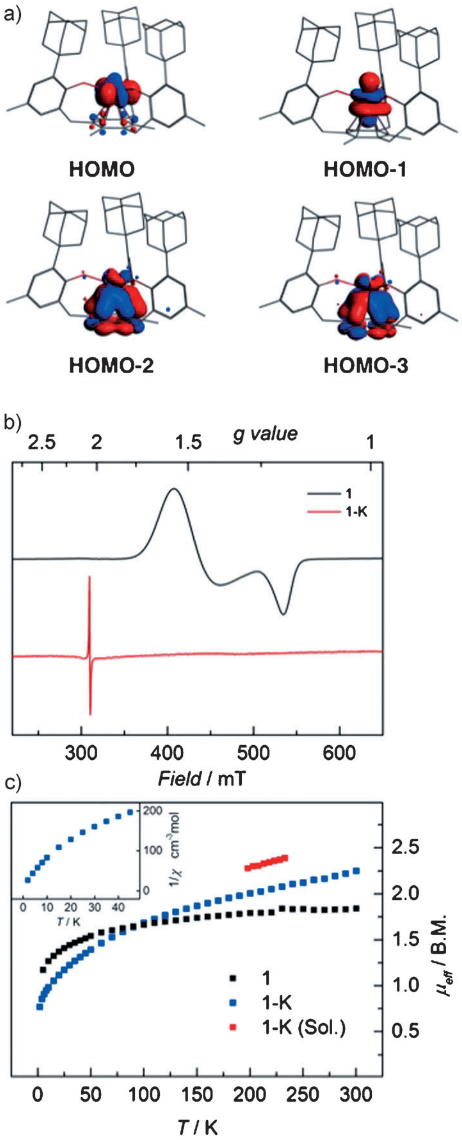

Figure 3. a) Representations of the four highest singly-occupied spinors of 1^- from DFT calculations with the BP functional, including spin-orbit coupling. The relative energetic ordering of the four spinors may differ with other exchange-correlation functionals as observed in corresponding scalar-relativistic calculations. b) X-band EPR spectra of **1** in toluene and **1-K** in THF at 20 K. See the Supporting Information for simulation and spectrometer parameters. c) Temperature-dependent SQUID magnetization data (at 1 T, 2–300 K) for **1** and **1-K**, plotted as a function of magnetic moment (μ_{eff})versus temperature, and the data from the temperature-dependent Evans' method for 15 mm **1-K** (198–233 K, bottom). $1/\chi$ v. T data for **1-K** plotted from 2–45 K (inset, see the Supporting Information for full T range).

configuration. However, the highest occupied spinor shows some constructive overlap of a U-centered f orbital with a high energy π* orbital of the η^6 bound arene ring. Hence, while the scalar DFT calculations on the full system 1^- suggest an essentially metal-centered reduction of **1** (see the Supporting Information), an inspection of the molecular orbitals and the properties of the relevant spinors of 1^- (including spin-orbit effects) point to a mixed arene and U-centered reduction (Figure 3 a).[25]

Experimental support for the predicted $S=2$, $5f^4$ ground state in **1-K** was obtained by X-band EPR. A spectrum of the uranium(III) precursor **1**, obtained at 20 K in toluene (Figure 3 b), displays an anisotropic, nearly axial signal indicative of a $^4I_{9/2}$ (U^{3+}, f^3) ion with a doublet electronic ground state. Simulation of the spectrum gives g values of 1.58, 1.46, and 1.20. Upon reduction, **1-K** is EPR silent as expected for a complex with a non-magnetic (or integer spin) ground state (Figure 3 b), whether it is a quintet or triplet state. The small signal observed at $g=2.00$ is due to solvated electrons supported by $[K(2.2.2\text{-crypt})]^+$ necessary to quantitatively generate **1-K** in the presence of excess potassium (see the Supporting Information for experimental details).[26]

Solid-state and solution-phase magnetism studies of **1-K** were also pursued. A non-standard method was required to obtain a powdered sample for SQUID analysis. The complex **1-K** was prepared in situ, as for the variable-temperature ^1H NMR and UV/vis experiments, with a slight excess of the 2.2.2-cryptand in THF at −35 °C with potassium spheres. This solution was then decanted and the THF removed in vacuo at less than −40 °C to give a powder that was briefly warmed to room temperature, massed, and then chilled prior to insertion into the SQUID. As a result, there is residual diamagnetic impurity resulting from the excess 2.2.2-cryptand and the observed magnetic moment is low. For **1-K**, at 300 K the effective magnetic moment, μ_{eff}, is 2.25 B.M. and decreases to 0.77 B.M. at 2 K (Figure 3 c). The weak temperature-dependent paramagnetism at very low temperature indicates an integer spin ground state (Figure 3 c, inset), which is in agreement with the EPR studies (i.e. EPR non-active). While there are no magnetism studies of U^{2+} complexes for comparison, similar behavior has been described for an octahedral $5f^4$, $^5I_4$ complex, $Cs_2[PuCl_6]$.[27]

In comparison to the precursor uranium(III) complex **1**, the reduced **1-K** clearly possesses divergent temperature-dependent paramagnetism at higher temperatures. Solution magnetism studies on **1-K**, performed using the method of Evans, between −40 °C and −75 °C, match the temperature dependency observed for the solid-state measurements and indicate that the observed solid-state magnetic behavior is from **1-K**. As a result of the inclusion of solvated electrons (as observed by EPR, vide supra), there is a residual paramagnetic impurity in the measurements from the Evans method and the observed magnetic moment is high (Figure 3 c).

In summary, the identification and comprehensive analysis of a new formal oxidation state of molecular uranium reveals the limitations of our knowledge about an element of central economic and cultural importance. These spectroscopic, crystallographic, magnetic, and theoretical studies on **1-K** indicate that a molecular uranium(II) complex with a $5f^4$, $^5I_4$ ground state can be stabilized by employing a δ-bonding arene within a chelating aryloxide ligand framework. Additionally the isolation and thorough characterization of **1-K** establish that the nearly reversible reduction of **1** at −2.495 V vs. Fc/Fc^+ is principally metal-centered. Future studies will explore the electronic structure of the complex by X-ray absorption techniques and its reactivity with small molecules.

Received: February 3, 2014
Published online: May 30, 2014

Keywords: arenes · electronic structure · magnetic properties · uranium · X-ray diffraction

[1] F. A. Cotton, G. Wilkinson, *Advanced Inorganic Chemistry*, 2nd ed., Wiley-Interscience, New York, **1966**.

[2] a) J. Blaise, J.-F. Wyatt, *International Tables of Selected Constants, Vol. 20*, **1992**; b) W. J. Liu, W. Kuchle, M. Dolg, *Phys. Rev. A* **1998**, *58*, 1103; c) X. Y. Cao, M. Dolg, *Mol. Phys.* **2003**, *101*, 961; d) B. A. Palmer, R. Engleman, *J. Opt. Soc. Am.* **1984**, *1*, 609.

[3] a) W. C. Martin, R. Zalubas, L. Hagan, *Atomic Energy Levels—The Rare-Earth Elements, the Spectra of La, Ce, Pr, Nd, Pm, Sm, Eu, Gd, Tb, Dy, Ho, Er, Tm, Yb, Lu*, National Bureau of Standards, U.S. Department of Commerce, Washington, DC, **1978**; b) M. R. MacDonald, J. E. Bates, J. W. Ziller, F. Furche, W. J. Evans, *J. Am. Chem. Soc.* **2013**, *135*, 9857.

[4] a) L. Andrews, M. F. Zhou, B. Y. Liang, J. Li, B. E. Bursten, *J. Am. Chem. Soc.* **2000**, *122*, 11440; b) B. Y. Liang, L. Andrews, N. Ismail, C. J. Marsden, *Inorg. Chem.* **2002**, *41*, 2811.

[5] E. D. Eastman, L. Brewer, L. A. Bromley, P. W. Gilles, N. L. Lofgren, *J. Am. Chem. Soc.* **1950**, *72*, 4019.

[6] A. B. Mclaren, B. Kanellakopulos, E. Dornberger, *Inorg. Nucl. Chem. Lett.* **1980**, *16*, 223.

[7] a) J. M. Manriquez, P. J. Fagan, T. J. Marks, S. H. Vollmer, C. S. Day, V. W. Day, *J. Am. Chem. Soc.* **1979**, *101*, 5075; b) P. J. Fagan, J. M. Manriquez, T. J. Marks, C. S. Day, S. H. Vollmer, V. W. Day, *Organometallics* **1982**, *1*, 170; c) B. P. Warner, B. L. Scott, C. J. Burns, *Angew. Chem.* **1998**, *110*, 1005; *Angew. Chem. Int. Ed.* **1998**, *37*, 959; d) W. J. Evans, S. A. Kozimor, *Coord. Chem. Rev.* **2006**, *250*, 911.

[8] R. G. Finke, G. Gaughan, R. Voegeli, *J. Organomet. Chem.* **1982**, *229*, 179.

[9] a) P. L. Diaconescu, P. L. Arnold, T. A. Baker, D. J. Mindiola, C. C. Cummins, *J. Am. Chem. Soc.* **2000**, *122*, 6108; b) W. J. Evans, S. A. Kozimor, J. W. Ziller, N. Kaltsoyannis, *J. Am. Chem. Soc.* **2004**, *126*, 14533.

[10] a) P. L. Diaconescu, C. C. Cummins, *J. Am. Chem. Soc.* **2002**, *124*, 7660; b) P. L. Diaconescu, C. C. Cummins, *Inorg. Chem.* **2012**, *51*, 2902; c) W. J. Evans, C. A. Traina, J. W. Ziller, *J. Am. Chem. Soc.* **2009**, *131*, 17473; d) M. J. Monreal, S. I. Khan, J. L. Kiplinger, P. L. Diaconescu, *Chem. Commun.* **2011**, *47*, 9119; e) D. P. Mills, F. Moro, J. McMaster, J. van Slageren, W. Lewis, A. J. Blake, S. T. Liddle, *Nat. Chem.* **2011**, *3*, 454; f) V. Mougel, C. Camp, J. Pecaut, C. Coperet, L. Maron, C. E. Kefalidis, M. Mazzanti, *Angew. Chem.* **2012**, *124*, 12446; *Angew. Chem. Int. Ed.* **2012**, *51*, 12280; g) D. Patel, F. Moro, J. McMaster, W. Lewis, A. J. Blake, S. T. Liddle, *Angew. Chem.* **2011**, *123*, 10572; *Angew. Chem. Int. Ed.* **2011**, *50*, 10388; h) D. Patel, F. Tuna, E. J. L. McInnes, J. McMaster, W. Lewis, A. J. Blake, S. T. Liddle, *Dalton Trans.* **2013**, *42*, 5224; i) H. S. La Pierre, K. Meyer, *Prog. Inorg. Chem.* **2014**, *58*, 303.

[11] B. Vlaisavljevich, P. L. Diaconescu, W. L. Lukens, L. Gagliardi, C. C. Cummins, *Organometallics* **2013**, *32*, 1341.

[12] a) M. R. MacDonald, J. W. Ziller, W. J. Evans, *J. Am. Chem. Soc.* **2011**, *133*, 15914; b) M. R. MacDonald, J. E. Bates, M. E. Fieser, J. W. Ziller, F. Furche, W. J. Evans, *J. Am. Chem. Soc.* **2012**, *134*, 8420.

[13] a) P. C. Blake, N. M. Edelstein, P. B. Hitchcock, W. K. Kot, M. F. Lappert, G. V. Shalimoff, S. Tian, *J. Organomet. Chem.* **2001**, *636*, 124; b) M. C. Cassani, D. J. Duncalf, M. F. Lappert, *J. Am. Chem. Soc.* **1998**, *120*, 12958; c) P. B. Hitchcock, M. F. Lappert, L. Maron, A. V. Protchenko, *Angew. Chem.* **2008**, *120*, 1510; *Angew. Chem. Int. Ed.* **2008**, *47*, 1488.

[14] M. R. MacDonald, M. E. Fieser, J. E. Bates, J. W. Ziller, F. Furche, W. J. Evans, *J. Am. Chem. Soc.* **2013**, *135*, 13310.

[15] H. S. La Pierre, H. Kameo, D. P. Halter, F. W. Heinemann, K. Meyer, *Angew. Chem.* **2014**, DOI: 10.1002/ange.201402048; *Angew. Chem. Int. Ed.* **2014**, DOI: 10.1002/anie.201402048.

[16] a) W. J. Evans, S. A. Kozimor, W. R. Hillman, J. W. Ziller, *Organometallics* **2005**, *24*, 4676; b) W. G. Van Der Sluys, C. J. Burns, J. C. Huffman, A. P. Sattelberger, *J. Am. Chem. Soc.* **1988**, *110*, 5924; c) D. Baudry, E. Bulot, P. Charpin, M. Ephritikhine, M. Lance, M. Nierlich, J. Vigner, *J. Organomet. Chem.* **1989**, *371*, 155; d) D. Baudry, E. Bulot, M. Ephritikhine, *J. Chem. Soc. Chem. Commun.* **1988**, 1369; e) A. V. Garbar, M. R. Leonov, L. N. Zakharov, Y. T. Struchkov, *Russ. Chem. Bull.* **1996**, *45*, 451; f) G. C. Campbell, F. A. Cotton, J. F. Haw, W. Schwotzer, *Organometallics* **1986**, *5*, 274; g) F. A. Cotton, W. Schwotzer, C. Q. Simpson, *Angew. Chem.* **1986**, *98*, 652; *Angew. Chem. Int. Ed. Engl.* **1986**, *25*, 637; h) F. A. Cotton, W. Schwotzer, *Organometallics* **1985**, *4*, 942; i) M. Cesari, U. Pedretti, A. Zazzatta, G. Lugli, W. Marconi, *Inorg. Chim. Acta* **1971**, *5*, 439.

[17] a) S. C. Bart, F. W. Heinemann, C. Anthon, C. Hauser, K. Meyer, *Inorg. Chem.* **2009**, *48*, 9419; b) O. P. Lam, S. C. Bart, H. Kameo, F. W. Heinemann, K. Meyer, *Chem. Commun.* **2010**, *46*, 3137.

[18] The broadening of the resonances of the cryptand is due to the slight excess of cryptand and the presence of solvated electrons supported by $[K(2.2.2\text{-crypt})]^+$. See EPR discussion in text and in the Supporting Information.

[19] a) R. Ahlrichs, M. Bar, M. Haser, H. Horn, C. Kolmel, *Chem. Phys. Lett.* **1989**, *162*, 165; b) R. Ahlrichs, F. Furche, C. Hattig, W. M. Klopper, M. Sierka, F. Weigend, Turbomole program package, version 6.3, University of Karlsruhe; http://www.turbomole.com; c) G. te Velde, F. M. Bickelhaupt, S. J. A. van Gisbergen, C. F. Guerra, E. J. Baerends, J. G. Snijders, T. Ziegler, *J. Comput. Chem.* **2001**, *22*, 931; d) E. J. Baerends, et al., Amsterdam Density Functional package (ADF), version 2013.01; http://www.scm.com.

[20] a) K. Boguslawski, C. R. Jacob, M. Reiher, *J. Chem. Theory Comput.* **2011**, *7*, 2740; b) The role of spin in DFT has nicely been summarized by Jacob and Reiher recently. See: C. R. Jacob, M. Reiher, *Int. J. Quantum Chem.* **2012**, *112*, 3661.

[21] a) W. Kuchle, M. Dolg, H. Stoll, H. Preuss, *J. Chem. Phys.* **1994**, *100*, 7535; b) X. Y. Cao, M. Dolg, *J. Mol. Struct. (THEOCHEM)* **2004**, *673*, 203; c) E. van Lenthe, E. J. Baerends, J. G. Snijders, *J. Chem. Phys.* **1993**, *99*, 4597.

[22] E. van Lenthe, J. G. Snijders, E. J. Baerends, *J. Chem. Phys.* **1996**, *105*, 6505.

[23] a) J. M. Tao, J. P. Perdew, V. N. Staroverov, G. E. Scuseria, *Phys. Rev. Lett.* **2003**, *91*, 146401; b) A. D. Becke, *Phys. Rev. A* **1988**, *38*, 3098; c) J. P. Perdew, *Phys. Rev. B* **1986**, *33*, 8822; d) A. D. Becke, *J. Chem. Phys.* **1993**, *98*, 5648; e) P. J. Stephens, F. J. Devlin, C. F. Chabalowski, M. J. Frisch, *J. Phys. Chem.* **1994**, *98*, 11623; f) V. N. Staroverov, G. E. Scuseria, J. M. Tao, J. P. Perdew, *J. Chem. Phys.* **2003**, *119*, 12129.

[24] S. M. Franke, B. L. Tran, F. W. Heinemann, W. Hieringer, D. J. Mindiola, K. Meyer, *Inorg. Chem.* **2013**, *52*, 10552.

[25] Inspection of the partial charges (see Tables S10 and S11 in the Supporting Information) suggests that the reduction event, while principally metal-centered, also involves a rearrangement of charge between the uranium ion and the arene ligand.

[26] A. S. Ichimura, M. J. Wagner, J. L. Dye, *J. Phys. Chem. B* **2002**, *106*, 11196.

[27] D. G. Karraker, *Inorg. Chem.* **1971**, *10*, 1564.

[28] CCDC 994192 (**1-K**) and 994193 for (**2**) contain the supplementary crystallographic data for this paper. These data can be obtained free of charge from The Cambridge Crystallographic Data Centre via www.ccdc.cam.ac.uk/data_request/cif.